

## CHAPTER 2

### Literature Review

#### 2.1 Ferroelectric materials in general

Ferroelectric materials are a special example of polar materials which can show an electric phenomenon called the ferroelectric effect or ferroelectricity, that is, it exhibits a spontaneous electric dipole moment (this is similar to ferromagnetic—showing a permanent magnetic moment). Moreover, its spontaneous electric polarization  $P_s$  (electric dipole moment per unit volume) can be reversed or oriented in direction by a suitably strong applied electric field [6]. Typically, ferroelectric materials show a succession of phase transitions from high-temperature high-structural-symmetry paraelectric phase into low-temperature low-structural-symmetry ferroelectric phase. A more familiar example of ferroelectric materials is barium titanate,  $\text{BaTiO}_3$ . It can undergo several phase transitions into successive ferroelectric phases. A certain phase transition temperature is called the Curie temperature  $T_C$ . Above this phase transition temperature, the electric polarization  $P$  can arise only when an external electric field  $E$  is imposed. Materials are in a paraelectric phase. Below this temperature, the centroids of the positive charges and the negative charges do not coincide, so there is a net electric polarization even in the absence of an external electric field. They are in a ferroelectric phase.

A ferroelectric material that transforms from a paraelectric cubic into a ferroelectric tetragonal phase is shown in Figure 2.1. This phase transition is accompanied by changes in the dimensions of the crystal unit cell. These changes are called the spontaneous strain  $x_s$  which is the relative difference in dimensions of the ferroelectric unit cell ( $a_T$  and  $c_T$ ) and paraelectric unit cell ( $a_C$ ). Moreover, some ferroelectric materials, like barium titanate, can undergo several phase transitions into successive ferroelectric phase.

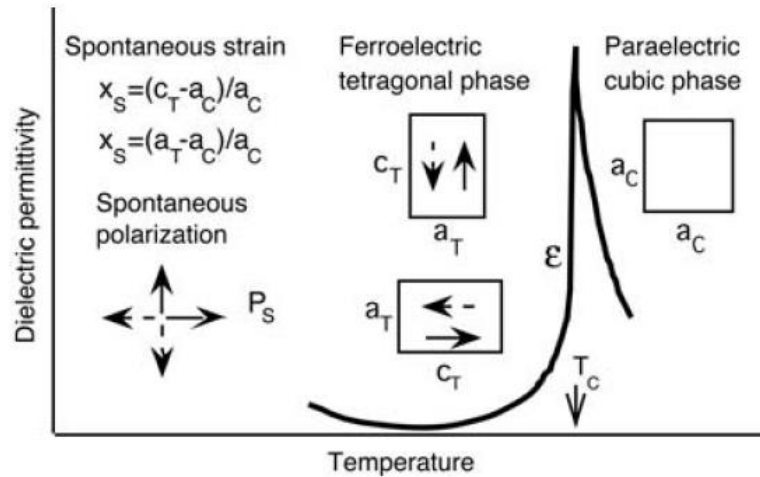


Figure 2.1 A succession of phase transition of a ferroelectric material [6].

Ferroelectric materials have tiny regions with a uniform electric polarization called ferroelectric domains. All electric dipoles of each domain align in the same direction. Ferroelectric materials can exhibit a hysteresis loop as shown in as shown in Figure 2.2. There is a residual polarization when an applied electric field is removed, it is called the remnant polarization,  $+P_r$  or  $-P_r$ . To reverse the direction of polarization, we need to apply an electric field called a coercive electric field,  $+E_c$  or  $-E_c$ , (a minimum electric field for switching the polarization).

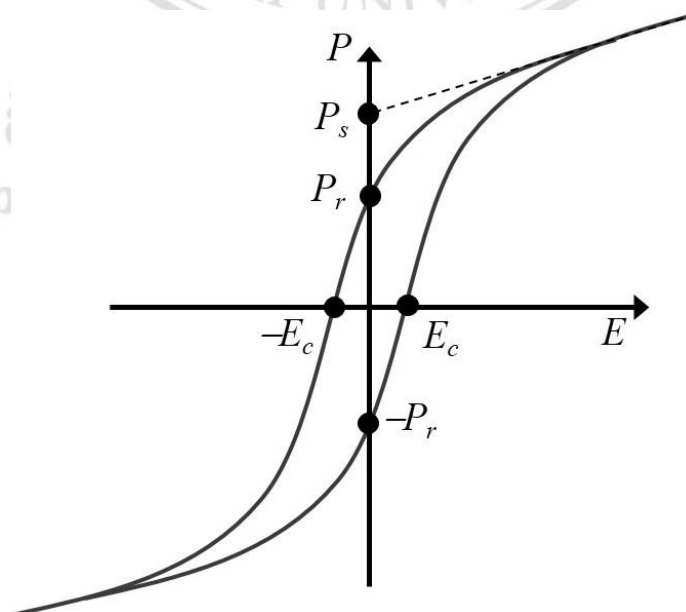


Figure 2.2 A hysteresis ferroelectric loop.

The polarization-electric field ( $P$ - $E$ ) hysteresis loop is an important property of ferroelectric materials. It has become an interesting of intensive studies due to potential applications of ferroelectric thin films in nonvolatile memories. Since the data in ferroelectric memories are stored in term of positive or negative remnant polarization state and this state can be controlled by reversing the polarization's direction from up (+1) to down (-1) or vice versa as a function of applied electric field, the most studies have focused on particular applications such as the difference between the positive and negative remnant polarization,  $P_r - (-P_r)$ , the dependence of the coercive electric field  $E_c$  on sample thickness  $l$ , or so on. Moreover, most electronic devices rely on various important properties of ferroelectric materials as shown in Figure 2.3.

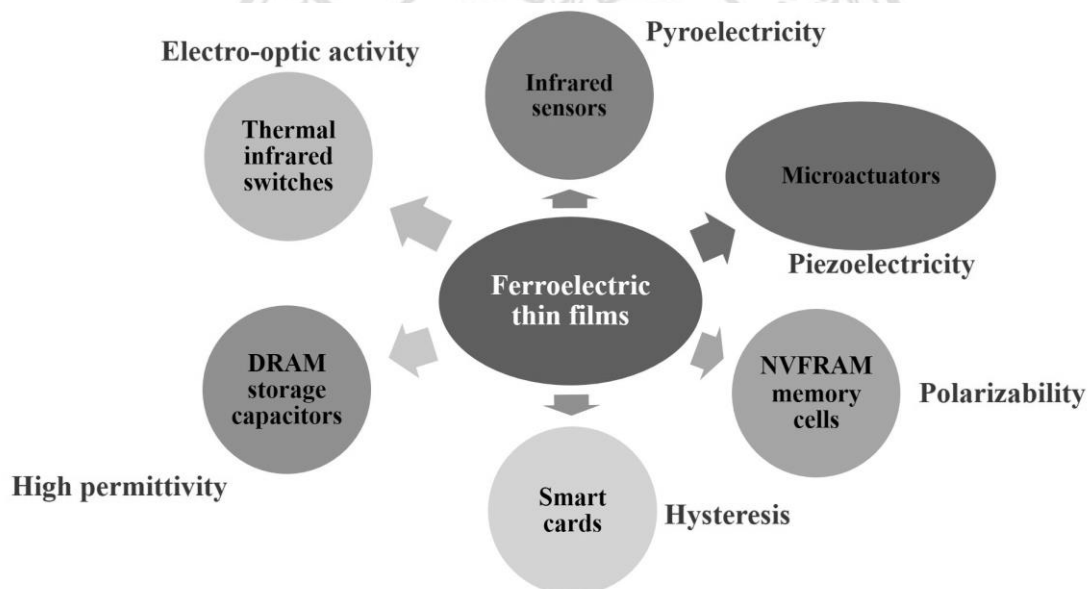


Figure 2.3 Ferroelectric thin films and applications.

A Hysteresis loop can be characterized by a history-independent path. It naturally occurs in many physical systems under some circumstances such as the application and the removal of an external electric field, an external magnetic field, or a stress field. It also exhibits the non-linearity properties and phase transitions of physical systems. A time-dependent electric polarization is found to be lag behind a time-dependent external electric field, and a polarization-electric field ( $P$ - $E$ ) hysteresis loop occurs. Moreover, a phase transition is also accompanied by changes in a unit cell. The associated changes are called the spontaneous strain  $\epsilon_s$ . Therefore, the polarization switching by a time-dependent oscillatory external electric field in ferroelectric materials may lead to a

strain-electric field ( $\varepsilon$ - $E$ ) hysteresis loop even in with or without a mechanical stress field  $\sigma$ . This hysteresis loop, which is similar to a butterfly shape, is called a butterfly loop.

## 2.2 Ferroelectric hysteresis area

It is usually found that the ferroelectric hysteresis properties depend on the external perturbations, such as the field frequency  $f$ , field amplitude  $E_0$ , and temperature  $T$ . The period average polarization  $Q$  are generally investigated and the dynamic phase transition diagram can be obtained. In general, in order to empirically obtain how hysteresis loop area  $A$  relates to these perturbations, the power-law scaling is usually performed in many experimental and theoretical studies of ferroelectric materials [23-29]. For instance, a hysteresis loop area can be written as

$$A \propto f^\alpha E_0^\beta T^\gamma \quad (2.1)$$

where  $\alpha$ ,  $\beta$ , and  $\gamma$  are exponents to the scaling. Then, the exponents can be estimated, and the power-law dependency on external perturbations of the hysteresis loop area. However, the obtained exponents depend on the considered parameter range. For example, in BaTiO<sub>3</sub> ceramics, above and under the coercive field  $E_C$  the hysteresis loop area scaling is in the forms of  $A \propto f^{-0.23} E_0^{0.87}$  and  $A \propto f^{-0.36} E_0^{3.64}$  respectively [30]. Moreover, the exponents cannot be predicted in the region close to the turning point (where the scaling function has to change from power-law growth to power-law decay). Consequently, some important hysteresis behaviors cannot be predicted by power-law scaling. Fourier analysis is another method that can be used to find the relations between the hysteresis loop area and field parameters of ferroelectric materials [31].

In microscopic view, fundamental analysis, such as the spin model, the mean-field approach and Monte Carlo simulation, is proposed to study the dynamic ferroelectric behaviors in details (this analysis seeks for the understanding of nature from microscopically inside out), and data processing analysis, such as the artificial neural network (ANN) and Fourier analysis, is used to link experimental results with external perturbations empirically. In general, data processing analysis is used to find a connection between the macroscopic phenomena and experimental conditions.

### 2.3 Spin models

A spin model is a mathematical model used widely in studying the dynamic properties of magnetic materials at the microscopic scale. The considered magnetic material consists of many magnetic dipole moments called spins. Under a time-dependent external magnetic field, the Hamiltonian of spin system is given as [32]:

$$H = -\sum_{\langle ij \rangle} J_{ij} \mathbf{s}_i \cdot \mathbf{s}_j + \sum_{ij} K_{ij} \left[ \frac{\mathbf{s}_i \cdot \mathbf{s}_j}{r_{ij}^3} - \frac{(\mathbf{s}_i \cdot \mathbf{r}_{ij})(\mathbf{s}_j \cdot \mathbf{r}_{ij})}{r_{ij}^5} \right] + \sum_i (D_i \cdot \mathbf{s}_i)^2 - \sum_i \mathbf{h}(t) \cdot \mathbf{s}_i \quad (2.2)$$

where  $J_{ij}$  represents the exchange interaction between spin vector  $\mathbf{s}_i$  and  $\mathbf{s}_j$ ,  $D_i$  denotes the anisotropic interaction,  $K_{ij}$  refers to dipolar interaction strength, and  $\mathbf{h}(t)$  is a time-dependent oscillating external magnetic field. The symbol  $\langle ij \rangle$  indicates that sum takes only the first neighbor pairs. By absorbing the unit of  $s_i$  into  $J_{ij}$ ,  $K_{ij}$ ,  $D_i$  and  $\mathbf{h}(t)$ , therefore,  $J_{ij}$ ,  $K_{ij}$ ,  $D_i$  and  $\mathbf{h}(t)$  can be used as a unit of energy. Further, the spin models can be classified into two subgroups—discrete and continuous spin models. The examples of well-known discrete spin models are the Ising model and the Potts model as well as the DFFOUR model, while the two most widely studied models of continuous spin models are the XY model and the Heisenberg model [33].

Starting with the simplest spin model, i.e. the Ising model, each Ising spin is allowed to have only 2 possible directions on one axis e.g. the  $z$ -axis. Therefore,  $s_i = s_i \hat{z} = \pm 1 \hat{z}$  as  $s_i$  can be only  $\pm 1$ . Typically, the  $z$ -direction is chosen to be the easy axis direction or the applied external field direction. If the field is periodic in time and on the  $z$ -direction, it is possible to choose  $\mathbf{h}(t) = h_0 \sin(\omega t) \hat{z}$  where  $h_0$  and  $\omega$  are the field amplitude and field frequency, respectively. For an isotropic case and consider only the strongest interaction, it is possible to choose  $K_{ij} = D_i = 0$  and  $J_{ij} = J$  where  $J$  is the ferromagnetic ( $J > 0$ ) and antiferromagnetic exchange interaction ( $J < 0$ ), respectively. Therefore, from Equation (2.2), the Ising Hamiltonian can be written as

$$H = -J \sum_{\langle ij \rangle} s_i s_j - \sum_i h(t) s_i \quad (2.3)$$

where  $h(t) = h_0 \sin(\omega t)$ . On the other hand, the Potts model is another discrete spin

model, but its spin can take more discrete values, that is,  $s_i = 1, 2, 3, \dots, q$  where  $q$  is the maximum state a spin can have. Note that the Potts model is equivalent to the Ising model when  $q = 2$  [33]. Additionally, an improved version of the Potts model is the DIFFOUR model which is usually used to study the ferroelectric dynamics behaviors.

Unlike the discrete-spin models, e.g. the Ising or the Potts model, the XY model provides spin as two-component vector of unit length and can point to any directions on a two-dimensional plane, that is,  $\vec{s}_i = (\cos \theta_i, \sin \theta_i)$ . Therefore,  $\vec{s}_i \cdot \vec{s}_j$  can be replaced by  $\cos \theta_{ij}$ , where  $\theta_{ij}$  is an angle between the two spins. It should be noted that although XY spins are two-dimensional vector, but they can be also used in the three-dimensional spatial-system. The Heisenberg model has a same concept as the XY model, but the spins are three-dimensional unit vector, and can be represented by two angles of spherical coordinate— $\phi$  and  $\theta$  i.e.,  $\vec{s}_i = (\sin \theta_i \cos \phi_i, \sin \theta_i \sin \phi_i, \cos \theta_i)$  [33].

Apart from the ferromagnetic subject, the basic idea of spin models can also be applied to study the dynamic hysteresis behaviors of ferroelectric materials. In ferroelectric spin systems,  $P$ - $E$  loops can be obtained using Monte Carlo simulation on the DIFFOUR model. In many previous works, the DIFFOUR model was successfully used to investigate the dynamic ferroelectric hysteresis [34-36]. For example, ferroelectric hysteresis properties in thin films were investigated using the DIFFOUR model with the Metropolis algorithm. It was found that their hysteresis properties, such as the hysteresis area, remnant polarization and coercivity field, depend on the film-thickness, frequency and amplitude of the field. Moreover, the DIFFOUR model can be considered in a special material, such as acceptor-doped ferroelectric material [37]. The obtained hysteresis profiles agreed well with experimental results. The concepts of the DIFFOUR model can be described as the following. Based on the DIFFOUR model, the Hamiltonian can be written as [36, 38]

$$H = \sum_i \left( \frac{P_0^2}{2m} - \frac{a}{2} u_i^2 + \frac{b}{2} u_i^4 \right) - \sum_{\langle ij \rangle} U_{ij} \vec{u}_i \cdot \vec{u}_j - \sum_i \vec{E}(t) \cdot \vec{u}_i \quad (2.4)$$

where  $P_0^2 / 2m$  is the kinetic energy,  $\vec{u}_i$  is the ferroelectric dipole (polarization) at site  $i$ ,  $a$  and  $b$  are the double-well potential parameters,  $\langle ij \rangle$  means that only nearest

neighbors pairs are taken into the sum,  $U_{ij}$  refers to the ferroelectric interaction and  $\vec{E}(t) = E_0 \sin(2\pi ft)\hat{z}$  is the time-dependent electric-field along one axis, e.g. the  $z$ -axis. In Equation (2.4), the first summation is the Landau free energy, the second summation represents the electrical dipole-dipole energy, and the last summation is the external electric field energy. In many previous works,  $a$  and  $b$  were set as constants with the condition  $a/b < 1$ , such as  $a/b = 0.1$  [35, 39] or  $a/b = 0.5$  [40, 41]. This is to satisfy the Landau phase transition between ferroelectric and paraelectric phase. In the Landau theory,  $a$  is proportional to temperature away from the critical point, that is,  $a \propto (T_c - T)$ . Therefore, close the critical point, or  $a/b = 1$ , the Landau theory gives a solution of  $u_i^2 = a/b$  under the absence of external electric field which is found to agree with mean field solutions [42]. As a result, although the ratio  $a/b$  changes, but as long it is small enough, the qualitative ferroelectric behavior close to the critical point should remain the same. Spin models can be discussed through the mean-field approach and Monte Carlo method.

#### 2.4 Mean-field theory

In mean-field theory, each local electric polarization,  $P$ , aligning in an effective electric field can be calculated from all surrounding electric dipole moments where fluctuations can be neglected, that is,

$$P = \frac{1}{N} \left\langle \sum_i^N u_i \right\rangle, \quad (2.5)$$

where  $u_i$  is the electric dipole moment and  $N$  denotes the number of electric dipole moment. Within the mean-field framework and ferroelectric system, the equation of motion for the average polarization  $P(t)$  is given by [43]:

$$\tau \frac{dP(t)}{dt} = -P(t) + \tanh \beta \left[ E(t) + \sum_i J_i P(t) \right], \quad (2.6)$$

where  $u_i$  is the microscopic relaxation time. From this approach, we can extract electric polarization under time-dependent electric field, or predict phase transition and explain behaviors of materials near the critical temperatures.

However, the mean-field method overestimates  $T_c$  and reports critical-exponent values do not depend on system dimensionality [44]. These are the weak points of the mean-field method caused by neglecting important fluctuation near the phase transition. On the other hand, Monte Carlo method is one of powerful tools in studying statistical physical problems, including phase transition and critical phenomena topics.

## 2.5 Monte Carlo method

The basic concept behind Monte Carlo simulation is to use stochastic process to take the system from one state into another possible state. The system can then pass through series of states with well-defined set of probabilities at a given time.

### 2.5.1 Probability theory

Consider an elementary event  $Q$ , such as a coin is tossed three times, with a countable set of all possible random outcomes,  $Q_1, Q_2, \dots, Q_k$ . If this event  $Q$  and the outcome  $Q_k$  occur  $N$  and  $N_k$  times repeatedly, the probabilities  $p_k$  for the outcome  $Q_k$  is

$$p_k = \lim_{N \rightarrow \infty} (N_k / N), \quad (2.7)$$

where  $\sum_k p_k = 1$ . In general the outcomes are also random variables. We define the expectation value of this random variable as follows:

$$\langle Q \rangle = \sum_k p_k Q_k. \quad (2.8)$$

The  $n$ th moment of  $Q$  can be given by

$$\langle Q^n \rangle = \sum_k p_k Q_k^n, \quad (2.9)$$

and we define the so-called cumulants

$$\langle (Q - \langle Q \rangle)^n \rangle = \sum_k p_k (Q_k - \langle Q \rangle)^n. \quad (2.10)$$

For  $n = 2$ , we obtain a well-known quantity called the **variance** or **fluctuation**,  $\sigma^2$ , i.e.



$$\sigma^2 = \langle (Q - \langle Q \rangle)^2 \rangle = \langle Q^2 \rangle - \langle Q \rangle^2 \quad (2.11)$$

The square root of the variance is called the **standard deviation**,  $\sigma$ , that is, we have

$$\sigma = \sqrt{\langle Q^2 \rangle - \langle Q \rangle^2} \quad (2.12)$$

We define the statistical error as follows:

$$\text{statistical error} = \frac{\sigma}{\sqrt{N}} \quad (2.13)$$

### 2.5.2 The estimator and important sampling

In statistical physics, we deal with systems with many degrees of freedom. One task is to compute the average or expectation of macroscopic observables from the total energy or Hamiltonian  $H$  for a thermal equilibrium system. For example, we may explain a magnetic system by the Ising model with uniaxial anisotropic spins as

$$H_{\text{Ising}} = -\sum_{\langle ij \rangle} J_{ij} S_i^z S_j^z - H \sum_i S_i^z, \quad (2.14)$$

where  $S_i^z$  means the spin pointing up (+1) or down (-1) along the  $z$ -axis or easy axis at site  $i$  on the lattice,  $J_{ij}$  is the exchange interaction between spin  $S_i^z$  and  $S_j^z$ ,  $\sum_{\langle ij \rangle} [\dots]$  refers to the sum over all pairs of nearest neighbor spins, and  $H$  is a magnetic field. However, if each spin can lie only in the  $xy$  plane or is fully isotropic, we may describe our magnetic systems by the  $XY$  model or Heisenberg model [45]:

$$H_{XY} = -\sum_{\langle ij \rangle} J_{ij} (S_i^x S_j^x + S_i^y S_j^y) - H_x \sum_i S_i^x, \quad (S_i^x)^2 + (S_i^y)^2 = 1, \quad (2.15)$$

$$H_{\text{Heisenberg}} = -\sum_{\langle ij \rangle} J_{ij} (\mathbf{S}_i \cdot \mathbf{S}_j) - H_z \sum_i S_i^z, \quad (S_i^x)^2 + (S_i^y)^2 + (S_i^z)^2 = 1. \quad (2.16)$$

Consider a thermal equilibrium system in contact with a reservoir at an absolute temperature  $T$ , the probability that system is in a microstate  $\mu$  is determined by the normalized Boltzmann factor, i.e.

$$p_k = \frac{e^{-\beta H_k}}{Z}, \quad (2.17)$$

where  $\beta = 1/k_B T$ ;  $k_B$  is the Boltzmann constant,  $H_k$  is the Hamiltonian of system in a given microstate  $k$ , and  $Z$  refers to a normalized constant called the **partition function**. The partition function includes all essential information about the system. For a classical system, the general form of the partition function,  $Z$ , is

$$Z = \sum_k e^{-\beta H_k}. \quad (2.18)$$

By replacing the probability  $p_k$  into Equation (2.8), we obtain the average of any observable  $Q$  for this system:

$$\langle Q \rangle = \frac{1}{Z} \sum_k Q_k e^{-\beta H_k}. \quad (2.19)$$

Equation (2.19) is suitable for the small systems. However, in larger systems, the number of possible different microstates is very large. We may choose only  $n$  independent states at random from some probability  $p_k$ . Equation (2.19) becomes

$$\langle Q \rangle \approx \bar{Q}_n = \frac{\sum_{\mu=1}^n Q_{\mu} p_{\mu}^{-1} e^{-\beta H_{\mu}}}{\sum_{\mu=1}^n p_{\mu}^{-1} e^{-\beta H_{\mu}}}, \quad (2.20)$$

where  $\bar{Q}_n$  is called the **estimator** of  $Q$ . The estimator becomes a more accurate estimate when  $n \rightarrow \infty$ ; we have  $\bar{Q}_n = \langle Q \rangle$ . In general, we choose  $p_{\mu}$  to have a simple and most natural form, that is,  $p_{\mu} \propto e^{-\beta H_{\mu}}$ , then the Boltzmann factor cancels out, top and bottom. Then Equation (2.20) reduces to a simple arithmetic expression:

$$\bar{Q}_n = \frac{1}{n} \sum_{\mu=1}^n Q_{\mu}, \quad (2.21)$$

A basic idea behind thermal Monte Carlo method is to pick out the important states from the very large number of probabilities. This process is called **important sampling**. Consequently, a good estimate can be obtained by choosing the sample of important  $n$  states and ignoring all the others. A sample of the state of the system will be picked

with its probabilities proportional to its Boltzmann factor. Then the estimator becomes a simple expression as Equation (2.21). Additionally, to choose each state with its correct Boltzmann probability, we perform a technique called a Markov process as described later.

### 2.5.3 Observables and fluctuation

We can write all thermodynamic quantities or observables in terms of the partition function. For example, from Equation (2.19), the internal energy  $U$  or the expectation value of the energy,  $\langle H \rangle$ , is given by

$$U = \langle H \rangle = \frac{1}{Z} \sum_k H_k e^{-\beta H_k} = -\frac{1}{Z} \frac{\partial Z}{\partial \beta} = -\frac{\partial \ln Z}{\partial \beta}. \quad (2.22)$$

Then, the specific heat  $C$  can be calculated from the internal energy, i.e.

$$C = \frac{\partial U}{\partial T} = -k_B \beta^2 \frac{\partial U}{\partial \beta} = k_B \beta^2 \frac{\partial^2 \ln Z}{\partial \beta^2}. \quad (2.23)$$

In addition, the (Helmholtz) free energy  $F$  of system can be also written in the terms of partition function, that is,

$$F = -k_B T \ln Z. \quad (2.24)$$

The expectation of the magnetization,  $\langle M \rangle$  and the magnetic susceptibility,  $\chi$ , can be obtained from the free energy  $F$ , that is,

$$\langle M \rangle = \frac{1}{Z} \sum_{\mu} M_{\mu} e^{-\beta H_{\mu}} = \frac{1}{\beta} \frac{\partial \ln z}{\partial B} = -\frac{\partial F}{\partial B}, \quad (2.25)$$

$$\chi = \frac{\partial}{\partial B} \langle M \rangle = -\frac{\partial^2 F}{\partial B^2}, \quad (2.26)$$

where  $B = -(1/M)H$ .

In practice, some observables such as the specific heat capacity and magnetic susceptibility can be written in terms of fluctuations, that is,

$$C = k_B \beta^2 (\langle U^2 \rangle - \langle U \rangle^2), \quad (2.27)$$

$$\chi = \beta (\langle M^2 \rangle - \langle M \rangle^2). \quad (2.28)$$

#### 2.5.4 Markov process

The Markov process is a discrete stochastic method with three basic properties: (1) the number of possible states is finite, (2) any stage depends only on previous or current state and (3) the probabilities are constant over time. These are **called Markov property**. A Markov process starts from a configuration  $\mu$  at time  $t$  and generate a new one  $\nu$  at time  $t + \Delta t$ . The evolution from state  $\mu$  to state  $\nu$  is governed by **transition probability**  $R(\mu \rightarrow \nu)$ . We further require that

$$R(\mu \rightarrow \nu) \geq 0, \quad \sum_{\nu} R(\mu \rightarrow \nu) = 1. \quad (2.29)$$

Each transition depends only on the current state of the system and not on the previous history. Normally, we assume that the transition probability is time-independent.

Let  $p_{\mu}(t)$  be the probability that the system will be in state  $\mu$  at time  $t$ . The probability  $p_{\mu}(t)$  must also satisfy this relation:

$$\sum_{\mu} p_{\mu}(t) = 1. \quad (2.30)$$

We can write the **master equation** for the evolution of  $p_{\mu}(t)$  as [33]

$$\frac{dp_{\mu}(t)}{dt} = \sum_{\nu} [p_{\nu}(t)R(\nu \rightarrow \mu) - p_{\mu}(t)R(\mu \rightarrow \nu)]. \quad (2.31)$$

In a Monte Carlo simulation, the Markov process will generate a succession of states with the Boltzmann probabilities. In addition to the condition as Equation (2.30), we need two further conditions for our Markov process: ergodicity and detailed balance.

### 2.5.5 Ergodicity and detailed balance

Ergodicity is an important condition for our Markov process. The ergodicity condition tells us that all possible configurations of the system should be accessible, if we run the process for long enough: although some other state may have zero transition probability, but there should exist at least a path of non-zero transition probabilities connecting two arbitrary states  $\mu$  and  $\nu$ , that is,  $\mu \rightarrow \alpha \rightarrow \beta \rightarrow \dots \rightarrow \nu$ . Any algorithm created in the Monte Carlo simulation should satisfy the ergodicity condition, such as the Metropolis or Wolff algorithm.

Detailed balance is another condition required in our Markov process. This condition makes us ensure when the system is in equilibrium, we should create the Boltzmann probability distribution rather than any other distribution. As the system is in equilibrium, we obtain  $dp_\mu(t)/dt = 0$ , then Equation (2.31) becomes

$$p_\nu R(\nu \rightarrow \mu) = p_\mu R(\mu \rightarrow \nu). \quad (2.32)$$

This is the detailed balance condition which says that the probability of system moving from a state  $\mu$  to another one  $\nu$  is equal to that of system moving a state  $\nu$  to another one  $\mu$ . However, if we choose  $p_\mu$  to be the equilibrium distribution or Boltzmann distribution, we can obtain the detailed balance condition as

$$\frac{R(\mu \rightarrow \nu)}{R(\nu \rightarrow \mu)} = \frac{p_\nu}{p_\mu} = e^{-\beta(E_\nu - E_\mu)}. \quad (2.33)$$

Equation (2.33) tell us that, at thermal equilibrium, the ratio of transition probabilities for moving state  $\mu$  to state  $\nu$  and its inverse depends only on the energy difference between new state and old state, e.g.  $E_\nu - E_\mu$ . Therefore, we need these conditions: ergodicity and detailed balance conditions, to make the probability distribution in our Markov process be the Boltzmann distribution as desired.

### 2.5.6 The Metropolis algorithm

The normalization condition  $\sum_\nu R(\mu \rightarrow \nu) = 1$  in Equation (2.29) includes the transition probability  $R(\mu \rightarrow \mu)$ , which means the absence of transition. We find that

when  $\nu = \mu$ , Equation (2.32) gives  $1 = 1$ , that is, the detailed balance is always valid for any  $R(\mu \rightarrow \mu)$ . Thus we can set the transition probability to any values as desired. In general, we split the transition probability as follows:

$$R(\mu \rightarrow \nu) = g(\mu \rightarrow \nu)A(\mu \rightarrow \nu), \quad (2.34)$$

where  $g(\mu \rightarrow \nu)$  and  $A(\mu \rightarrow \nu)$  are the selection probability and acceptance ratio, respectively.

The selection probability says in our algorithm which state can be generated from a given old state. Suppose there are  $N$  spins in our Ising model with single spin flip update, we can generate a new state by choosing a spin at random out of  $N$  different spins. In this case the selection probability is

$$g(\mu \rightarrow \nu) = \frac{1}{N}. \quad (2.35)$$

This equation is always valid for its inverse. From Equations (2.34) and (2.35), the detailed balance condition becomes

$$\frac{R(\mu \rightarrow \nu)}{R(\nu \rightarrow \mu)} = \frac{g(\mu \rightarrow \nu)A(\mu \rightarrow \nu)}{g(\nu \rightarrow \mu)A(\nu \rightarrow \mu)} = \frac{A(\mu \rightarrow \nu)}{A(\nu \rightarrow \mu)} = e^{-\beta(E_\nu - E_\mu)}. \quad (2.36)$$

The acceptance ratio is the fraction of times that the actual transition takes place. Thus if  $E_\mu < E_\nu$ , we can set  $A(\nu \rightarrow \mu)$  to be one (the actual transition exists with the largest possible value). To satisfy Equation (2.36), we choose the following acceptance ratio:

$$A(\mu \rightarrow \nu) = \begin{cases} e^{-\beta(E_\nu - E_\mu)}; & \text{if } E_\nu > E_\mu \\ 1 & ; \text{ otherwise} \end{cases}. \quad (2.37)$$

Equation (2.37) says we always accept the transition to a new state if it has energy lower than or equal to the old one. However if it has a higher energy, we can accept the transition with the acceptance ratio as Equation (2.37).

### 2.5.7 Equilibrium and measurement

In general, when we choose an initial state at random, our system may take a long time before it has come to equilibrium at a temperature interested. This time is called the equilibration time  $\tau_{eq}$ . To find  $\tau_{eq}$ , we plot some physical quantities interested as a function of time. When thermal equilibrium reaches, these quantities begin to fluctuate around a steady average value. The question is “How long does a system come to equilibrium?” Firstly, we need to define the unit of time. Time is measured in Monte Carlo step per lattice site (MCS). For our system with the total number of spins  $N$  on the lattice, one MCS refers to one sweep lattice (in other words,  $N$  steps altogether) in the Metropolis algorithm or one single cluster-flip in the Wolff algorithm. To make sure our system has come to equilibrium, at least we choose the equilibration time to be the total number of spins on the lattice, that is,  $\tau_{eq} = N$  [33].

Once our system has reached equilibrium, we need to measure the observables interested, such as the energy and the magnetization. In the Metropolis algorithm, if we know the current energy  $E_\mu$ , we can find the new energy  $E_\nu$  when we flip a spin:

$$E_\nu = E_\mu - \Delta E, \quad (2.38)$$

where  $\Delta E$  is the energy difference in moving from state  $\mu$  to state  $\nu$ . To calculate efficiently, we should find the energy of system at the beginning of simulation and calculate the new energy every time we flip a spin from Equation (2.38).

### 2.6 Data processing analysis

Fundamental analysis is an appropriate method used to investigate the nature behaviors of materials. However, due to the complexity of materials, it is too difficult to this approach. Data processing analysis is a very direct way to set up the relationship between input and output parameters without the need to get the fundamental knowledge. Mostly data processing analysis is used for designing extensive database for specific ranges of input for easy and quick prediction of the output. The examples of this analysis are Artificial Neural Network and Fourier transformation.

### 2.6.1 Artificial Neural Network

The Artificial Neural Network (ANN) is a computer model consisting of a number of processing element or ‘artificial neurons’ inspired by the real human neurons in the brain. In the human brain, when a neuron receives a strong enough signal, it is activated and emits the signal to adjacent neurons, and the signal is linked to a recognized perception taken from pool of experiences. In the same manner, each artificial neuron behaves as a processing unit which receives inputs (usually more than one) and transform to input-weighted-sum  $a = \sum_{\text{all inputs}} x_i w_i$ , where  $x_i$  is an input signal and  $w_i$  is signal weight. To compute the output, an activation function  $f$  is applied on  $a$ , then the output  $f(a)$  is obtained as illustrated in Figure 2.4.

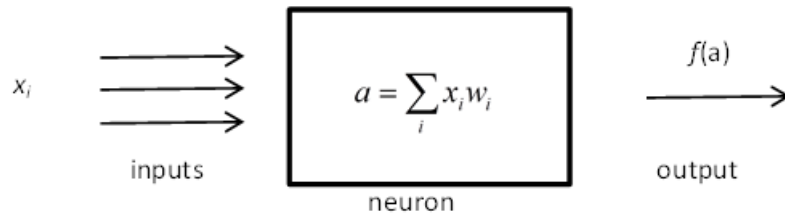


Figure 2.4 Input signals, an input-weighted-sum and an output signal of a neuron [46].

One of the most commonly used activation functions is

$$f(x) = \frac{1}{1 + e^{-cx}}, \quad (2.39)$$

where  $x = a$  and  $c$  is a positive scaling constant. In performing ANN modeling, artificial neurons are organized in layers as shown in Figure 2.5 [46], where the first layer on the left hand side is the input layer. Input data are fed to the network through this layer. Outputs from ANN are obtained from the output layer on the right hand side. The layers between input and output are called the hidden layers. There may be one or more hidden layers between an input and output layers. Neurons in each layer are connected together (indicated by lines connecting between neurons). The strength of the connection is indicated by signal weight ( $w_i$ ). In Figure 2.5, the field frequency, field amplitude, or temperatures are provided in the input layer and the corresponding hysteresis area is obtained from the output layer. However, if preferred, there could be more than one



output in the output layer, such as hysteresis area, remnant magnetization, coercive field, and etc.

During the ANN processing, the signal weights  $w_i$  are adjusted to minimize the error between the network outputs and desired outputs. The weight adjustment process is called ‘training’ which is governed by the learning algorithm. One of most well-known learning algorithms is the Back Propagation (BP) algorithm [47, 48]. The idea of the BP algorithm can be described as the following. The training begins with assigning small random number to all signal weights. Then two stages calculation is performed. Firstly, in the ‘forward pass’ input data are presented to the network, and then output from each neurons are calculated using input-weighted-sum  $a$  and Equation (2.39) to obtain the final outputs in the output layer. These outputs are then compared with actual output, and the deviation or error are determined. Secondly, the ‘backward pass’ is performed by adjusting all signal weights in order to minimize the error. These two stages calculation are repeated with the new set of input-output examples until the stopping criterion is met, and the weights are kept for ANN prediction.

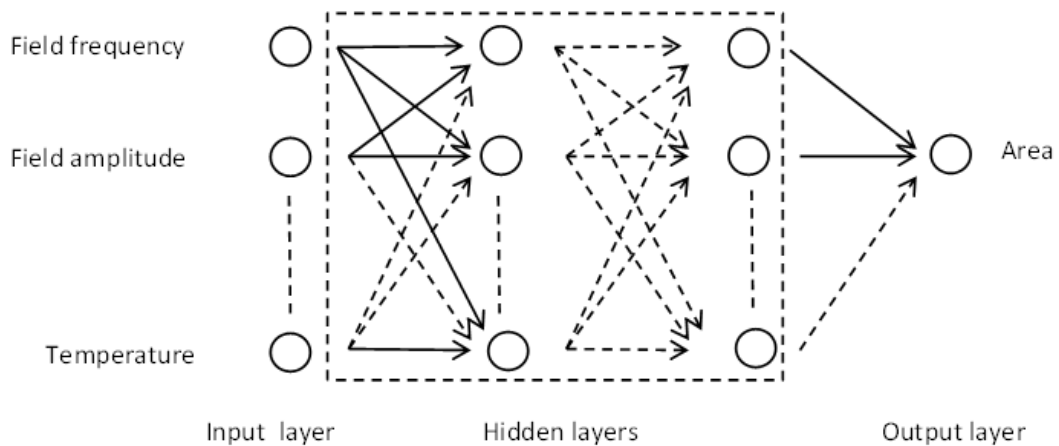


Figure 2.5 An example of schematic diagram for ANN modeling of ferroelectric hysteresis area [46].

The ANN model has been efficiently applied to many works in physics and materials science [47, 49-52], manufacturing [53, 54] and business [55, 56]. For example, an ANN model was used in modeling ceramics-powder preparation in obtaining the pure perovskite phase [50]. It was also used to find the complex relation between ferroelectric hysteresis properties and external electric field parameters [52], Example

of how accurate the ANN is in hysteresis modeling can be found in Ref. [57], where the predicted and the real hysteresis areas were found to agree well over the considered parameter ranges. As can be seen, this truly reflect advantages of using ANN modeling as dynamic hysteresis behavior can be illustrated without the comprehension of how dynamic hysteresis behaviors depend on the applied perturbation and complex internal interaction in the system.

## 2.6.2 Fourier transformation

In Fourier transformation, any periodic function in time domain  $f(t)$  can be expressed as the sum of sine and cosine series, that is,

$$f(t) = \frac{1}{2}a_0 + \sum_i a_i \cos(\omega_i t) + \sum_i b_i \sin(\omega_i t); \quad i = 1, 2, 3, \dots \quad (2.40)$$

where  $a_0$ ,  $a_i$  and  $b_i$  are Fourier coefficients,  $\omega_i$  is the  $i^{\text{th}}$ -order frequency, and  $t$  is time. Fourier transformation is an alternative method that can be used to model the dynamic hysteresis behaviors. However, since hysteresis data are discretely measured at a time interval  $\delta t$ , the time domain parameter  $t$  has to be represented by the data-point domain  $n$ . For instance, by taking hysteresis loop of BaTiO<sub>3</sub> bulk ceramics as an application [31], we can show the electric field and polarization as a function of data-point and the original field dependence of polarization, or  $P$ - $E$  hysteresis loop [57]. In order to change the data from data-point domain  $n$  to the frequency domain  $k$ , Fourier transformation is given as [31, 58, 59]

$$F(k) = \sum_{n=0}^{N-1} f(n)e^{-i2\pi nk/N}, \quad (2.41)$$

which can be written as

$$F(k) = \sum_{n=0}^{N-1} f(n) \cos(2\pi nk / N) - i \sum_{n=0}^{N-1} f(n) \sin(2\pi nk / N) = a_k - ib_k \quad (2.42)$$

where  $N$  is the number of data points in one field period,  $a_k$  and  $b_k$  are the Fourier coefficients or the amplitudes of  $k^{\text{th}}$  harmonic of real and imaginary part, respectively. Then, by applying Equation (2.42) to ferroelectric hysteresis of BaTiO<sub>3</sub> bulk ceramics,

$k^{\text{th}}$  harmonic amplitudes of real and part imaginary parts of the polarization signal can be shown as a previous work [31]. As can be seen, all even harmonics are small due to the almost symmetric behavior of the hysteresis loop. Therefore even harmonics can be ignored, while odd harmonics become more pronounced, As a result, the hysteresis area can be calculated from

$$A = -\frac{2\pi}{N} E_0 a_1, \quad (2.43)$$

where  $a_1$  is the first-harmonic Fourier coefficient of real part and  $E_0$  represents the field amplitude. It was also found that the positive and negative remnant polarizations depend on all odd harmonic of real parts as

$$p_r^\pm = m \frac{2}{N} \sum_{n=1}^{N/2} a_n. \quad (2.44)$$

In addition, the positive and negative coercive field can be computed from the first harmonic amplitude of real and imaginary parts

$$E_c^\pm = \pm E_0 \sin[\tan^{-1}(a_1 / b_1)]. \quad (2.45)$$

To confirm their validities, the hysteresis area from Equation (2.43), the remnant polarizations from Equation (2.44) and coercive field from Equation (2.45) were compared those measured from the experiment, and were found to agree very well as shown in Table 2.1 [31, 46].

In fact, these hysteresis properties can be directly extracted from the original hysteresis. For instance, the hysteresis area can be calculated by performing the numerical integration methods e.g. trapezoidal or Simpsons methods. However, due to the electronic noise or poor experimental set up, the  $P$ - $E$  loop obtained from the experiment may be distorted, asymmetric, or unexpectedly shifted along  $P$ -axis or  $E$ -axis. These random or unwanted noises distort the hysteresis loop from its ideal shape. Consequently, this may concealed some important fundamental phenomena and may prohibit unbiased link between the true hysteresis properties and the external perturbation. Therefore, the Fourier transformation can be used to ease these problems.

Table 2.1 Comparison of ferroelectric hysteresis properties obtained from the Fourier prediction and real measurement [31, 46].

Observables	Fourier prediction	Real measurement
$A$ (mCV/cm <sup>3</sup> )	133.6468	133.5459
$\frac{P_r^+ - P_r^-}{2}$ ( $\mu\text{C}/\text{cm}^2$ )	8.1887	8.1887
$\frac{E_c^+ - E_c^-}{2}$ (kV/cm <sup>2</sup> )	3.4367	3.4594



ลิขสิทธิ์มหาวิทยาลัยเชียงใหม่  
 Copyright© by Chiang Mai University  
 All rights reserved